

Effect of interface intermixing on giant magnetoresistance in NiFe/Cu and Co/NiFe/Co/Cu multilayers

L. C. C. M. Nagamine^{a)}

Instituto de Física–UFRGS, C.P. 15051, 91501-970, Porto Alegre-RS, Brazil

A. Biondo

Centro Brasileiro de Pesquisas Físicas–CBPF, R. Dr. Xavier Sigaud 150, Urca, 2290-180, Rio de Janeiro-RJ, Brazil, and Departamento de Física–UFES, 29060-900, Vitória, ES, Brazil

L. G. Pereira

Instituto de Física–UFRGS, C.P. 15051, 91501-970, Porto Alegre-RS, Brazil

A. Mello

Centro Brasileiro de Pesquisas Físicas–CBPF, R. Dr. Xavier Sigaud 150, Urca, 2290-180, Rio de Janeiro-RJ, Brazil

J. E. Schmidt, T. W. Chimendes, and J. B. M. Cunha

Instituto de Física–UFRGS, C.P. 15051, 91501-970, Porto Alegre-RS, Brazil

E. B. Saitovitch

Centro Brasileiro de Pesquisas Físicas–CBPF, R. Dr. Xavier Sigaud 150, Urca, 2290-180, Rio de Janeiro-RJ, Brazil

(Received 13 June 2002; accepted 13 August 2003)

This article reports on the important influence of the spontaneously built-in paramagnetic interfacial layers on the magnetic and magnetoresistive properties of NiFe/Cu and Co/NiFe/Co/Cu multilayers grown by magnetron sputtering. A computational simulation, based on a semiclassical model, has been used to reproduce the variations of the resistivity and of the magnetoresistance (MR) amplitude with the thickness of the NiFe, Cu, and Co layers. We showed that the compositionally intermixed layers at NiFe/Cu interfaces, which are paramagnetic, reduce the flow of polarized electrons and produce a masking on the estimated mean-free path of both types of electrons due to the reduction of their effective values, mainly for small NiFe thickness. Moreover, the transmission coefficients for the electrons decrease when Fe buffer layers are replaced by NiFe ones. This result is interpreted in terms of the variations of the interfacial intermixing and roughness at the interfaces, leading to an increase of the paramagnetic interfacial layer thickness. The effect provoked by Co deposition at the NiFe 16 Å/Cu interfaces has also been investigated. The maximum of the MR amplitudes was found at 5 Å of Co, resulting in the quadruplication of the MR amplitude. This result is partially attributed to the interfacial spin-dependent scattering due to the increase of the magnetic order at interfaces. Another effect observed here was the increase of the spin-dependent scattering events in the bulk NiFe due to a larger effective NiFe thickness, since the paramagnetic interfacial layer thickness is decreased. © 2003 American Institute of Physics. [DOI: 10.1063/1.1615704]

I. INTRODUCTION

In the last years, the study of spin-valve structures (SPS) has received special attention due to their potential application in electronic devices. One of the most important SPS is the NiFe/Cu structure, which presents a good sensitivity (large magnetoresistance at low field) and promises to be a good candidate for application in magnetoresistive sensors. Although the presence of a paramagnetic interface layer produced by the intermixing of Cu in NiFe was observed in some works,^{1,2} detailed studies of the role of this layer on the transport properties are lacking. Speriosu *et al.*³ argued that the electron scattering within these layers, in spin valves, is not spin dependent and may include spin-flip scattering. It also contributes to the decrease of the flow of electrons

across the Cu spacer, effectively isolating the ferromagnetic layers from each other and, as a consequence, reduces the giant magnetoresistance. In contrast, Dieny^{4,5} assumed perfect transmission coefficients through the NiFe/Cu interfaces for both species of electrons in NiFe/Cu. However, they only obtained good fits for both magnetoresistance amplitudes and resistivity data (using a semiclassical resistivity model), when an anisotropy in the electron mean-free path was assumed, which was ascribed to the scattering at the boundaries of the columnar-shaped grains with their column axes perpendicular to the film plane. Therefore, they argue that the resistivity is more sensitive to the in-plane mean-free path and the magnetoresistance to the perpendicular mean-free path for the majority electrons.

Diao *et al.*⁶ have discussed the role of the buffer layer in determining the antiferromagnetic coupling and magnetoresistance of NiFeCo/Cu multilayers. They pointed out that the

^{a)}Electronic mail: nagamine@if.ufrgs.br

increase of magnetoresistance (MR) is associated with the increase of the transverse crystalline grain size due to the presence of Fe buffer layer. As compared to the multilayer grown directly on the Si substrate, the one grown on Fe buffer layer presented a decrease of the resistivity that was associated to the reduction of the grain boundary regions, where the electron scattering is not spin dependent. However, for a sample grown on a Zr buffer layer, a similar decrease of resistivity was also observed, although the grain size has not been changed so much. In addition, Parkin *et al.*^{7,8} have observed a large increase of the giant magnetoresistance (GMR) via the addition of thin Co interfacial layers in NiFe/Cu multilayers. The large increase of the MR has been qualitatively justified in terms of the enhancement of interface spin-dependent scattering.

In order to investigate in more details the role of interfacial Co layers, and try to elucidate the controversy on the influence of the paramagnetic layer on the transmission coefficients at interfaces and on the bulk spin-dependent scattering, we have carried out a more-detailed study on the magnetic, structural, and magnetoresistive properties of the NiFe/Cu and Co/NiFe/Co/Cu multilayers. From a more quantitative point of view, the dependences of both resistivity and magnetoresistance on NiFe and Co thicknesses have been analyzed using a semiclassical theory. In contrast to some works,^{4,5} which assume an anisotropy of mean-free path for the spin majority electrons within the ferromagnetic layers, our experimental results have been fitted taking into account that the paramagnetic interface layers can decrease the flow of electrons at interfaces, as suggested by Speriosu *et al.*³ The role of an Fe or NiFe buffer layer, and the introduction of Co layers at interfaces are discussed here as being a function of changes in the paramagnetic interfacial layers. Possible grain size change effects are also discussed.^{9,10}

The technique used to prepare the samples and experimental details are described in Sec. II. Section III is dedicated to describing the theoretical semiclassical model and the parameters used to fit the data. Section IV is divided into five parts: (a) analysis of the x-ray reflectivity data; (b) evaluation of the influence of the Cu layer thickness (t_{Cu}) on the coupling between the NiFe layers; (c) the effect of the replacement of Fe buffer layers by NiFe ones; (d) analysis of the NiFe thickness (t_{NiFe}) on the GMR amplitude, saturation field, and GMR sensitivity; and (e) the influence of the Co thickness (t_{Co}) at NiFe/Cu interfaces on the GMR amplitude, saturation field, and on the behavior of the interface layers. Section V is dedicated to the conclusions.

II. EXPERIMENTAL DETAILS

The multilayers were prepared by magnetron sputtering at room temperature (RT) in an AJA sputter deposition system, and were deposited onto polished Si(100) substrates covered with native SiO₂. The base pressure was 5.0×10^{-8} Torr and the Ar pressure during deposition was 2.0 mTorr. The distance between the targets and the substrates was fixed to 10.3 cm. The substrates were attached to a rotating arm controlled by a step motor and a shutter, located between the target and the substrates, that allowed the con-

trol of the deposition time. The Cu, Co, and Fe were dc sputtered at a rate of 1.2, 2.0, and 1.8 Å/s, respectively, while the NiFe was rf sputtered at 1.0 Å/s. These deposition rates were obtained by the analysis of low-angle x-ray scans. We deliberately chose to rf sputter NiFe in virtue of its enhanced structural quality as compared to dc sputter, as shown by Cowache *et al.*¹¹

We have deposited sequentially 54 Å of NiFe (or 90 Å of Fe) as a buffer layer, after that (NiFe $t_{\text{NiFe}}/\text{Cu}$ 9 Å)₂₀ or (Co/NiFe $t_{\text{NiFe}}/\text{Co}/\text{Cu}$ 9 Å)₂₀ multilayers (for $11 \text{ Å} \leq t_{\text{NiFe}} \leq 85 \text{ Å}$ and $1 \text{ Å} \leq t_{\text{Co}} \leq 7 \text{ Å}$), and finally, 16 Å of NiFe as a cap layer. The multilayer thicknesses were later checked by the analysis of the x-ray reflectivity. High angle diffraction scans were also performed for some of the multilayers on the same X-Pert Phillips $\theta-2\theta$ diffractometer (Cu $K\alpha$ radiation) employed in the low angle x-ray reflectivity.

The field-dependent magnetization was measured with an alternating gradient force magnetometer. The in-plane magnetoresistance data were extracted using an ac four-point-probe method (at the frequency of 16 Hz and ac current amplitude ~ 1 mA) at RT, and with the magnetic field applied orthogonal to the current. Conversion electron Mössbauer spectroscopies (CEMS) at RT were performed using a constant acceleration electromechanical drive system, a multichannel analyzer, and a He-CH₄ proportional counter.⁵⁷ Co in rhodium at RT was used as a Mössbauer source.

III. THEORETICAL MODEL

A numerical procedure, developed in the framework of a semiclassical model based on the Camley and Barnas approach,¹² was used in order to investigate the magnetotransport properties of spin-valve multilayers. For a given electrical field, the current is calculated by solving the Boltzmann equation according to the method developed by Pereira *et al.*¹³ Thus, the absolute value of the resistivity can be obtained for a multilayer using the analytical expression for the conductivity, which takes into account the spin-mixing effects (thermal effects). From the value of the resistivity in the parallel and antiparallel magnetic configurations, the GMR amplitude is deduced.

The analytical expression for the conductivity (σ_η) for the η th spin direction channel in a multilayer, with N individual layers, is given by the following expression:

$$\sigma_\eta = K \sum_i^N B_{\eta i} \left\{ \frac{4}{3} \Delta z_i - q_{\eta i} \sum_n^i c_{\eta i}^n (L_{i\eta}^{1,n} - L_{x\eta}^{2,n} + M_{i\eta}^{1,n} - M_{x\eta}^{2,n}) \right\},$$

$$L_{i\eta}^{m,n} = \left[\frac{1}{4} - \frac{5}{12} \Gamma_{i\eta}^{m,n} - \frac{1}{24} (\Gamma_{i\eta}^{m,n})^2 + \frac{1}{24} (\Gamma_{i\eta}^{m,n})^3 \right] e^{-\Gamma_{i\eta}^{m,n}}, \quad (1)$$

$$M_{i\eta}^{m,n} = \frac{(\Gamma_{i\eta}^{m,n})^2}{2} \left(1 - \frac{1}{12} (\Gamma_{i\eta}^{m,n})^2 \right) \int \frac{e^{-\Gamma_{i\eta}^{m,n} \mu}}{\mu} d\mu,$$

where

$$\begin{aligned}
 K &= \pi e^2 v_F^2 \frac{m^2}{\hbar^3}, \\
 \Delta z_i &= z_j - z_i, \\
 \Gamma_{i\eta}^{1,n} &= a_{\eta i}^n - q_{\eta i} z_j, \\
 \Gamma_{i\eta}^{2,n} &= a_{\eta i}^n - q_{\eta i} z_i \\
 x &= i - 1, \\
 j &= i + 1,
 \end{aligned} \tag{2}$$

and a and c are given by

$$\begin{aligned}
 a_{\eta 1}^1 &= 0, \\
 a_{\eta j}^1 &= z_i q_{\eta j}, \\
 a_{\eta j}^n &= a_{\eta i}^{n-1} + z_i (q_{\eta j} - q_{\eta i}), \\
 c_{\eta 1}^1 &= 1, \\
 c_{\eta j}^1 &= \psi_{i j \eta}, \\
 c_{\eta j}^n &= \beta_{i j \eta} c_{\eta i}^{n-1},
 \end{aligned} \tag{3}$$

and $q_{\eta i}$ and $B_{\eta i}$ are functions of the mean-free path, λ ,

$$\begin{aligned}
 q_{\eta i} &= -\frac{1}{\lambda_i^\uparrow} + \frac{1}{\lambda_i^{-\eta}} + \frac{2}{\lambda_i^\downarrow} - \sqrt{\left(\frac{1}{\lambda_i^\uparrow} - \frac{1}{\lambda_i^{-\eta}}\right)^2 + \left(\frac{2}{\lambda_i^\downarrow}\right)^2}, \\
 B_{\eta i} &= \frac{\frac{1}{\lambda_i^\uparrow} + \frac{2}{\lambda_i^\downarrow}}{\frac{1}{\lambda_i^\uparrow \lambda_i^{-\eta}} + \frac{1}{\lambda_i^\uparrow \lambda_i^\downarrow} + \frac{1}{\lambda_i^{-\eta} \lambda_i^\downarrow}}, \text{ and} \\
 \psi_{\eta i j} &= 1 - \beta_{\eta i j}, \\
 \beta_{\eta i j} &= Q_{\eta i} \frac{B_{\eta i}}{B_{\eta j}}.
 \end{aligned} \tag{4}$$

In these expressions, z_i is the thickness of an individual layer, e is the electron charge, m is the electron mass, v_F is the Fermi velocity, \hbar is the Planck constant, and $Q_{\eta i}$ is the interfacial transmission coefficient. The integral on the set of Eqs. (1) is the well-known exponential–integral function [$E_i(-x)$]. For more details about the model see Ref. 13.

The thermal dependence of the resistivity is split into two distinct contributions: bulk and interfacial resistivities. The temperature dependence of the bulk resistivity is given by a set of relations of the bulk resistivity ρ , spin–flip contribution $\rho^{\uparrow\downarrow}$, and the α coefficient ($\alpha = \rho^{\uparrow\downarrow}/\rho$). The first two parameters (ρ and $\rho^{\uparrow\downarrow}$) are extracted from the experimental data (see Ref. 13, and the references therein), and for the permalloy case, it was used $\rho_{\text{NiFe}} = \frac{2}{3}\rho_{\text{Fe}}$ and $\rho_{\text{NiFe}}^{\uparrow\downarrow} = \frac{2}{3}\rho_{\text{Fe}}^{\uparrow\downarrow}$. The relationship between ρ and λ is given by $\rho\lambda = \text{constant}$, and this constant, K' , is related with K [see expression (1)] by $K' = Kl$, where l corresponds to the total thickness of the multilayer. For the interface transmission coefficients, it was used the thermal evolution given by $Q(T) = Q(0) + \omega T^\gamma$ (see Ref. 14). In this work, the coefficients were set as $K = 1050 \pm 50$, $\omega = (13.0 \pm 0.6) \times 10^{-7}$, and $\gamma = 1.85 \pm 0.05$.

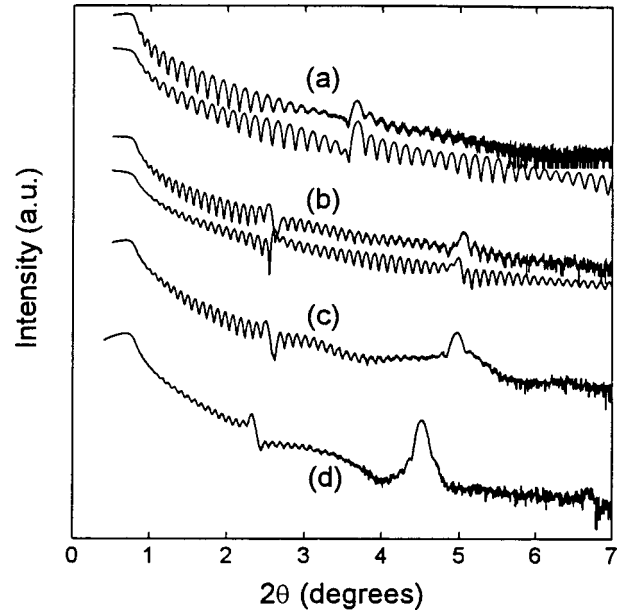


FIG. 1. Specular θ – 2θ x-ray diffraction for (NiFe 16 Å/Cu 9 Å)₂₀ (a), (Co 3 Å/NiFe 21 Å/Co 3 Å/Cu 9 Å)₂₀ (b), (Co 6 Å/NiFe 16 Å/Co 6 Å/Cu 9 Å)₂₀ (c), and (Co 7 Å/NiFe 16 Å/Co 7 Å/Cu 9.0 Å)₂₀ (d), where the upper line represents the measured data, the down line the simulation results. The curves have been displaced vertically for clarity.

The most important parameters in our simulations are: (a) the mean-free paths for each layer (λ), one for spin up (λ_\uparrow) and the other for spin down (λ_\downarrow); (b) the transmission coefficients at each interface (Q), Q_\uparrow for spin up and Q_\downarrow for spin down; and (c) the measurement temperature.

It is worth noting that in our calculations the parameters λ and Q represent physical characteristics of the multilayer. The mean-free paths describe the bulk scattering, which is determined by the bulk composition and/or disorder of the structure; the transmission coefficients correspond to the roughness, and the spin selective transmissions at the interfaces.

With a single set of parameters, we were able to fit the variation of the resistivity and of the MR amplitude as function of the thicknesses of the NiFe, Cu, and Co layers. Therefore, the parameters of the fitting were the mean-free paths in the NiFe, Cu, and Co layers and the transmission coefficients at (NiFe/Cu), (Cu/Co), or (Co/Cu) interfaces. The same computational procedure developed by Pereira *et al.*¹³ was also used by Dieny *et al.*¹⁴

IV. RESULTS AND DISCUSSION

A. X-ray reflectivity data

The program (WINGIXA) was employed to simulate (down lines in Fig. 1) the experimental reflectivity data (full lines, same figure), for (NiFe/Cu) and (Co/NiFe/Co/Cu) multilayers grown on NiFe buffer layer. One can note the presence of Kiessig fringes and one or two more pronounced peaks associated with the superlattice Bragg peaks. From the theoretical simulation, the layer structure was found to be Si/SiO₂ 28 Å/NiFe 54 Å/Cu 9 Å/(NiFe 16 Å/Cu 9 Å)₂₀/NiFe 16 Å [Fig. 1(a)], with the root-mean-square

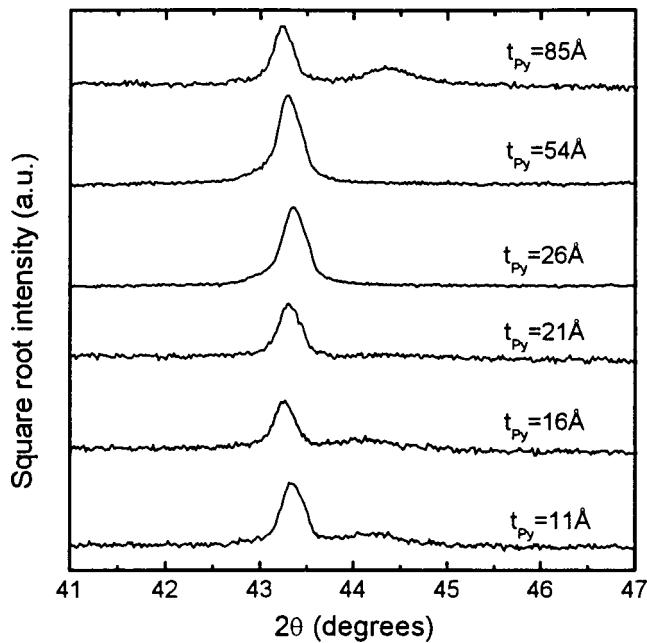


FIG. 2. High angle x-ray diffraction profiles for different NiFe layer thicknesses for the $(\text{NiFe } t_{\text{NiFe}}/\text{Cu } 9 \text{ \AA})_{20}$ series.

roughness of $(3 \pm 2) \text{ \AA}$ for the NiFe/Cu interfaces, and $(7 \pm 2) \text{ \AA}$ for the Cu/NiFe ones. A good agreement was found between the bilayer thickness determined from calibration rates (24.7 \AA), and the one obtained from reflectivity simulations (25 \AA).

The reflectivity data for the multilayer with approximately 1 ML of Co [Fig. 1(b)] were simulated using the stacking sequence, Si/SiO_2 $26 \text{ \AA}/\text{NiFe } 54 \text{ \AA}/\text{Cu } 9 \text{ \AA}/(\text{Co } 3 \text{ \AA}/\text{NiFe } 21 \text{ \AA}/\text{Co } 3 \text{ \AA}/\text{Cu } 9 \text{ \AA})_{20}/\text{NiFe } 16 \text{ \AA}$. For the NiFe/Co interfaces, the root-mean-square roughness is $(3 \pm 2) \text{ \AA}$, and $(5 \pm 2) \text{ \AA}$ for the Co/Cu interfaces. Attempts to fit these spectra with cumulative roughness throughout the stacking of the multilayer failed, so it can be concluded that this effect must be small or absent. As the lattice parameters and atomic scattering factors of NiFe, Cu, and Co are very close, these fitting curves are not so good. For this reason, the uncertainties on both layer thickness and roughness are large.

Although good fits have not been found for multilayers with thicker Co layers, the increase of roughness at the interfaces is evident from the broadening of the superlattice Bragg peaks, and from the loss of Kiessig fringes occurring at small angles [see Figs. 1(c) and 1(d)], as also demonstrated by Fullerton *et al.*¹⁵

The diffraction patterns for the NiFe/Cu series are displayed in Fig. 2. A clear (111) texture peak is observed for this series at $2\theta = 43.35^\circ$, an intermediate value between the Cu ($2\theta = 43.30^\circ$) and NiFe [it may vary from $2\theta_{(111)} = 43.47^\circ$, 39 at. % Ni (JCPDS, No. 23-0297) to 44.507° , Ni 100%]. The very broad and of small intensity peak for $t_{\text{NiFe}} = 85 \text{ \AA}$ can be associated with grains with higher Ni concentration. However, the high angle diffraction curve for the Co/NiFe/Co/Cu series, displayed in Fig. 3, shows a second Bragg peak at larger angles (near the Co fcc peak at $2\theta = 44.21^\circ$), due to a larger mismatch of Co on NiFe rather

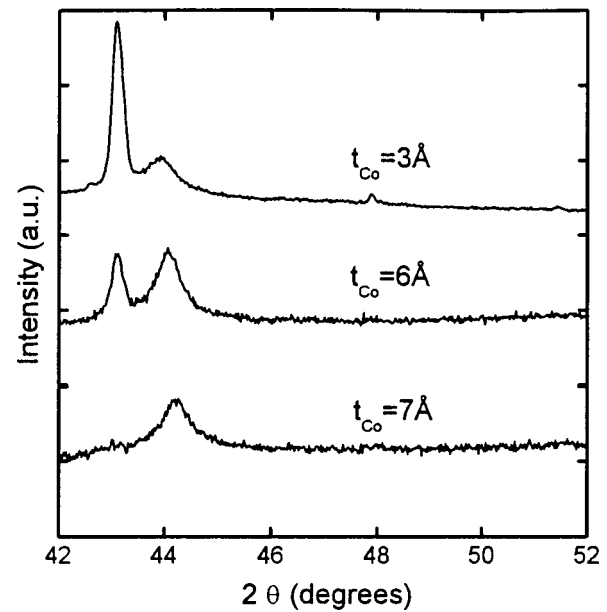


FIG. 3. High angle x-ray diffraction profiles for different Co layer thicknesses in the $\text{NiFe } 54 \text{ \AA}/\text{Cu } 9 \text{ \AA}/(\text{Co } t_{\text{Co}}/\text{NiFe } 16 \text{ \AA}/\text{Co } t_{\text{Co}}/\text{Cu } 9 \text{ \AA})_{20}/\text{Co } t_{\text{Co}}/\text{NiFe } 16 \text{ \AA}$ series.

than the mismatch of NiFe on Cu. The relative intensity of this peak has increased progressively with the Co thickness, until only this texture was observed for $t_{\text{Co}} = 7 \text{ \AA}$. This change in the microstructure is accompanied by an increase of interfacial roughness [see Fig. 1(d)], and, as a consequence, the MR amplitudes are negligible for the larger Co thickness, as will be shown later.

B. Influence of the thickness of the Cu spacer layers

A series of multilayers of the composition $\text{Fe } 90 \text{ \AA}/\text{Cu } t_{\text{Cu}}/(\text{NiFe } 16 \text{ \AA}/\text{Cu } t_{\text{Cu}})_{20}/\text{NiFe } 16 \text{ \AA}$ was prepared in order to study the influence of the Cu thickness on the magnetic and transport properties. Magnetoresistance data of this series are displayed in Fig. 4. A well-defined interval of Cu thicknesses (between 8 and 10 \AA) has been determined for which one observes an antiferromagnetic coupling between NiFe layers through the Cu layer (see Fig. 5). The saturation field has a maximum at 8 \AA of Cu, and then decreases monotonously to almost zero at 11 \AA of Cu. Using the two sets of data displayed in Fig. 5, one can find a rather good sensitivity S (0.015%/Oe) at 10 \AA of Cu, where $S = (\Delta R/R)/H_S$. It is worth noting that this Cu thickness does not correspond to the maximum of the GMR but is close to the upper edge of the MR plateau.

C. Influence of the buffer layer

To verify the effect of the buffer layers, as mentioned before, the case where $t_{\text{Cu}} = 9 \text{ \AA}$ (which corresponds to the maximum of the magnetoresistance) was chosen, and the Fe buffer layer was changed by the NiFe one. A large reduction of the interlayer coupling [see Fig. 6(a)], and a change of the saturation field from 3.5 to 1 kOe were observed. Although the magnetoresistance amplitude was reduced from 22% to 9.5% [see Fig. 6(b)], the sensitivity increased from 0.006 to

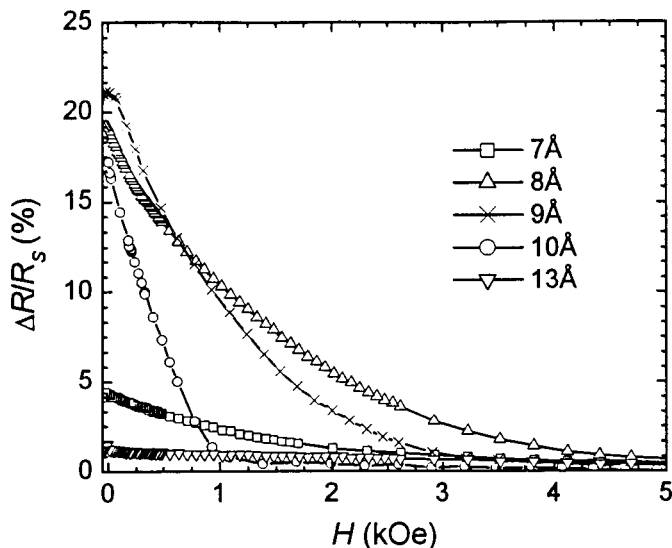


FIG. 4. Magnetoresistance at room temperature of a series of multilayers of composition Fe 90 Å/Cu t_{Cu} /(NiFe 16 Å/Cu t_{Cu})₂₀/NiFe 16 Å.

0.01%/Oe. The total remanent magnetization (normalized to the saturation magnetization) was 0.27, where approximately 67% of this value can be attributed to the NiFe buffer layer (0.18), and the rest to the existence of microscopic regions with ferromagnetic coupling (0.09). This incomplete antiferromagnetic coupling (~82%) reduces the spin valve effect.¹⁶ However, this effect is very weak in our samples and can be neglected in the theoretical model. For comparison, a higher normalized remanence of 0.39 was obtained for the case of the Fe buffer layer, which is largely attributed to this buffer layer [inset of Fig. 6(a)]. In part, the larger magnetoresistance amplitude found for the sample with Fe buffer layer can be attributed to a more complete antiferromagnetic coupling. Other possible factors will be discussed in the next section.

D. Influence of the thickness of the magnetic NiFe layers

A series of multilayers of composition NiFe 54 Å/Cu 9 Å/(NiFe t_{NiFe} /Cu 9 Å)₂₀/NiFe 16 Å with t_{NiFe} = 11,

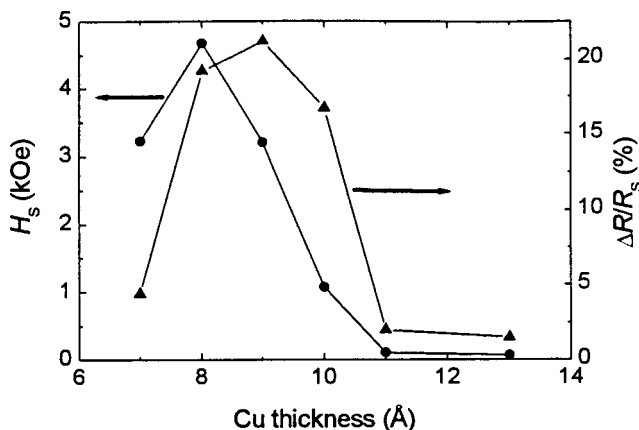


FIG. 5. Variation of the GMR amplitudes and the saturation field in a series of multilayers of composition Fe 90 Å/Cu t_{Cu} /(NiFe 16 Å/Cu t_{Cu})₂₀/NiFe 16 Å.

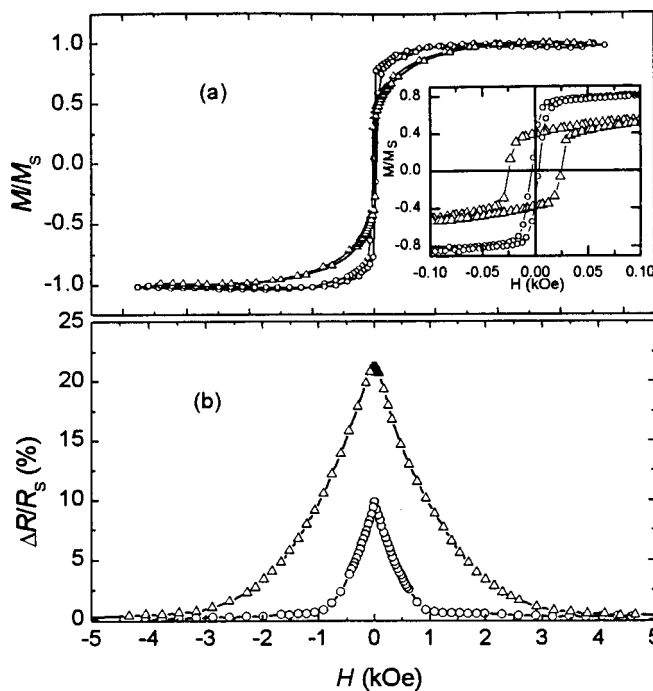


FIG. 6. Comparison of magnetic hysteresis curves (a) and magnetoresistance curves (b) of two samples of the same composition [buffer/Cu 9 Å/(NiFe 16 Å/Cu 9 Å)₂₀/NiFe 16 Å]; one has a buffer layer of 90 Å of Fe (triangles) while the other has a buffer layer of 54 Å of NiFe (circles). The inset in (a) represents the hysteresis loops at small fields.

16, 21, 26, 54, and 85 Å has been prepared. The magnetization and magnetoresistance curves are displayed in Figs. 7(a) and 7(b), respectively. The hysteresis loops for all samples show a clear ferromagnetic contribution, and saturate at relatively low fields. They also present a non-negligible remanent magnetization. Moreover, when one plots M/M_S vs H/H_S , the magnetization curves are very similar [see the inset of Fig. 7(a)]. This magnetic behavior means that both the bilinear and biquadratic magnetic couplings are independent of the NiFe thickness and all samples present almost the same ferromagnetic contribution. Such a similar ferromagnetic contribution is expected since both the buffer layer and Cu thickness are the same for all samples in this series.

The existence of both antiferromagnetic and non-negligible ferromagnetic couplings makes it very difficult to obtain the biquadratic and bilinear coefficients using the same procedure as given in Refs. 11 and 17. Despite that, as a consequence of the independency of these coefficients on the NiFe thickness, the saturation field is found to vary with the inverse of NiFe thickness, as shown in Fig. 8. Roughly, the bilinear coupling can be estimated from the following expression:¹⁸

$$H_S = \frac{4J}{M_S t_{NiFe}}, \tag{5}$$

where H_S is the saturation field, J is the bilinear coupling constant and M_S is the saturation magnetization. The slope of this line determines $J=0.018$ erg/cm² according to Eq. (5), which is in a good agreement with the value (0.020 erg/cm²) previously reported for NiFe/Cu multilayer by Parkin *et al.*,⁷ using $M_S=525$ emu/cm³ from Ref. 11.

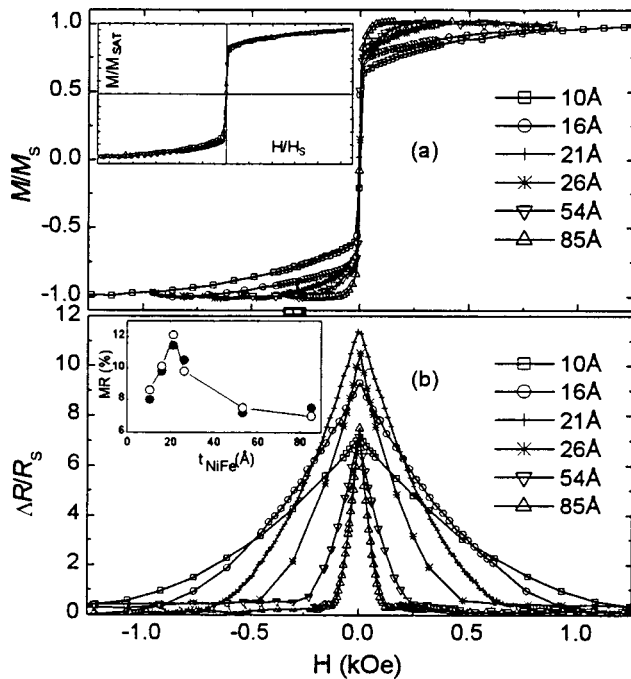


FIG. 7. (a) Magnetization curves at room temperature for a series of multilayers of the composition NiFe 54 Å/Cu 9 Å/(NiFe t_{NiFe} /Cu 9 Å)₂₀/NiFe 16 Å. The inset represents the same data plotted in reduced units M/M_S vs H/H_S showing the scaling behavior of these samples. (b) Magneto-resistance at room temperature for the same series of samples. The inset represents the GMR amplitude dependence on the NiFe thickness, where the full circles are the experimental results and open circles and lines are obtained from the fit.

The MR amplitudes as a function of NiFe thickness are shown as inset of Fig. 7(b), where full symbols represent the experimental data and the lines represent the fit; the parameter λ and Q of the fitting are displayed in Table I. The theoretical results for the series of (NiFe t_{NiFe} /Cu 9 Å)₂₀ (open circles + line) were obtained by using different parameters for each NiFe thickness. This procedure was justified by the presence of the paramagnetic layers at the interfaces,

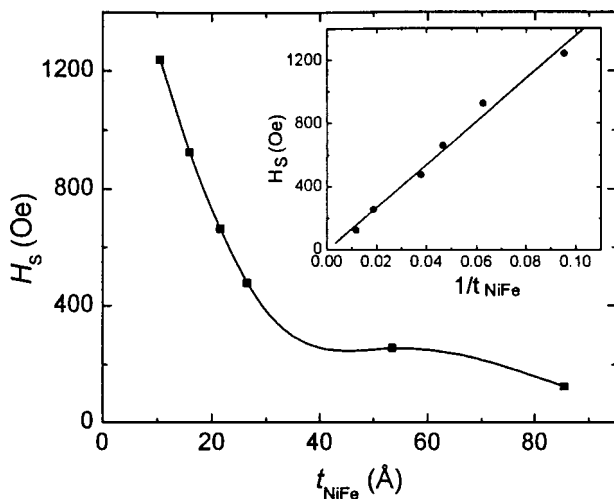


FIG. 8. Saturation field as a function of the NiFe layers for the same series of multilayers of the composition NiFe 54 Å/Cu 9 Å/(NiFe t_{NiFe} /Cu 9 Å)₂₀/NiFe 16 Å. The inset represents the saturation field vs $(t_{\text{NiFe}})^{-1}$.

TABLE I. Parameters deduced from the fit of both magnetoresistance and resistivity of a series of (NiFe t_{NiFe} /Cu 9 Å)₂₀. The mean-free paths for up and down electrons in the Cu layer are both 150 Å. The parameters of the temperature dependence are set as $K=1100$, $\omega=13 \times 10^{-7}$, and $\gamma=1.9$.

t_{NiFe} (Å)	10	16	21	26	54	85
λ_{\uparrow} (Å)	55	70	82	95	105	105
λ_{\downarrow} (Å)	3	3	3	12	14	5
Q_{\uparrow}	0.67	0.67	0.69	0.8	0.8	0.7
Q_{\downarrow}	0.61	0.61	0.61	0.8	0.8	0.7

that may be ascribed to some intermixing between NiFe and Cu. It is known that Ni has a strong tendency to exhibit a reduced magnetic moment or even to become nonmagnetic when it is alloyed with other nonmagnetic metals such as Cu, for instance.¹⁹ Moreover, for NiAg heterogeneous alloys, Nagamine *et al.*²⁰ have shown that intragrain magnetic fluctuation can play a significant role on the observed reduced magnetic moment.

In order to check the possible existence of a paramagnetic layer at NiFe/Cu interface in this series of samples, we carried out a study of conversion electron Mössbauer spectroscopy for (NiFe 54 Å/Cu 9 Å)₂₀. The spectra were fitted considering two hyperfine field distributions (Wevel-Mørup model²¹), one at small fields, which represents the interfacial paramagnetic phase, and the other at higher fields, representing the magnetic phase. The experimental and fitting spectra are displayed in Fig. 9. The normalized $P(H)$ distributions of each phase are shown as an inset in Fig. 9. Through the iron population of each magnetic phase, we estimated the thickness of the paramagnetic interfacial layer to be about (3 ± 1) Å. This result is in agreement with the value of 2.5 Å estimated by Lucinski *et al.* for a NiFe/Cu multilayer grown on Cu buffer layer.¹

Therefore, the NiFe/Cu interfacial alloy may be paramagnetic and can influence significantly both parameters, λ and Q , deduced from the fit, mainly for small thicknesses of NiFe, where the fraction of the paramagnetic layer is even more significant. These results also indicate an increase of the transmission coefficients for thicker layers of NiFe, probably due to the better structural quality of the interfaces for

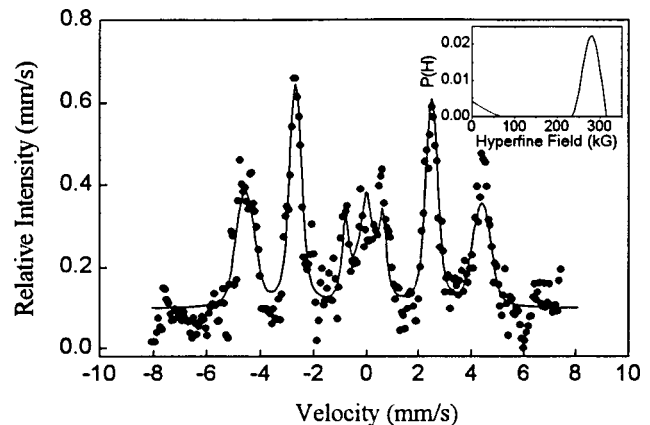


FIG. 9. CEMS spectra at room temperature for multilayers of composition NiFe 54 Å/Cu 9 Å/(NiFe 54 Å/Cu 9 Å)₂₀/NiFe 16 Å. The inset represents the relative population of each distribution function of hyperfine fields.

TABLE II. Experimental and theoretical resistivity at saturation of the series of (NiFe $t_{\text{NiFe}}/\text{Cu } 9 \text{ \AA}$)₂₀.

t_{NiFe} (Å)	10	16	21	26	54	85
ρ_{Exp} ($\mu\Omega$ cm)	50.1	47.5	45.5	36.2	34.0	36.6
ρ_{Fit} ($\mu\Omega$ cm)	50.2	48.2	45.1	36.1	34.0	36.8

these samples (see Fig. 2). The bulk spin-dependent scattering $\alpha = \lambda_{\uparrow}/\lambda_{\downarrow}$ is dominant, since $Q_{\uparrow} \approx Q_{\downarrow}$. The pair of values of λ obtained for samples with thicker layers of NiFe ($\lambda_{\uparrow} = 110 \text{ \AA}$, $\lambda_{\downarrow} = 5 \text{ \AA}$) is in agreement with the values reported by other authors.^{4,11,14}

The experimental and theoretical values of the resistivity for the parallel configuration are displayed in Table II. The agreement between experimental and theoretical resistivity values (parallel configuration) is quite good. The temperature variations (from 4.2 to 300 K) of the magnetoresistance and of the resistivity for these samples have been shown in another paper.²² Figure 7 shows a maximum of the GMR amplitude around 21 Å of NiFe thickness, whereas the sensitivity increases continuously from 0.006%/Oe ($t_{\text{NiFe}} = 11 \text{ \AA}$) to 0.06%/Oe ($t_{\text{NiFe}} = 85 \text{ \AA}$).

In order to better understand the MR results for multilayers with Fe or NiFe buffer layers [see Fig. 6(b)], we have also theoretically extracted the parameters for the multilayer with an Fe buffer, i.e., Si/Fe 90 Å/Cu 9 Å/(NiFe 16 Å/Cu 9 Å)₂₀/NiFe 16 Å. The experimental resistivity value decreased from 45.2 $\mu\Omega$ cm (NiFe buffer layer) to 29.3 $\mu\Omega$ cm (Fe buffer layer), and the theoretical parameters obtained for the sample with the Fe buffer layer ($\lambda_{\text{NiFe}}^{\uparrow} = 90 \text{ \AA}$, $\lambda_{\text{NiFe}}^{\downarrow} = 9 \text{ \AA}$, $Q_{\uparrow} = 1$, $Q_{\downarrow} = 1$), lead to a resistivity value of 29.1 $\mu\Omega$ cm, and 22.1% of MR amplitude, in very good agreement with the experimental values. A comparison of these parameters with the ones deduced for the same multilayer with a NiFe buffer layer (shown in Table I), allows us to observe the increase of the transmission coefficients of both types of electrons, and of the spin-dependent scattering in the bulk, when going from the first buffer to the second one. The increase of the transmission coefficients can be associated with the reduction of the paramagnetic interfacial layers. This factor can contribute to the larger MR amplitude found for the sample with the Fe buffer layer [see Fig. 6(b)], since the bulk spin-dependent scattering is enhanced.

In order to analyze the arguments that the grain size has a role to play depending on the buffer layer, the comments of Diao *et al.*⁶ are discussed here. They claim that the increase of the transverse grain size (in samples with an Fe buffer layer) results from the increase of the mean-free path of the majority electrons. To do this, the findings of Sun *et al.*²³ on the microstructure of Si/SiO₂/Fe 100 Å/(NiFe 15 Å/Cu 20 Å)₂₀ and glass/Fe 100 Å/(NiFe 13 Å/Cu 10 Å)₂₀ multilayers grown on a 100 Å Fe buffer layer through high-resolution transmission electron microscopy (HRTEM) were used. Columnar crystallites (CCs) were found to be the prominent structure, with average lateral sizes of 350 and 250 Å, respectively (see Fig. 1 of Ref. 23). As our multilayers have been fabricated with the same technique (magnetron

sputtering), and buffer layer (Fe) and NiFe and Cu layer thicknesses are approximately the same as their samples, we assumed that these grain sizes are suitable to aid us in evaluating their effects on our MR results and on the structural dependence of the parameters that we extract from the theory. In addition, an Fe 90 Å/Cu 20 Å/(NiFe 16 Å/Cu 20 Å)₂₀/NiFe 16 Å multilayer was also prepared, and a GMR amplitude of 8.9% and a resistivity value of 19.8 $\mu\Omega$ cm were measured for them. The theoretical parameters obtained in this case were: $\lambda_{\text{NiFe}}^{\uparrow} = 92 \text{ \AA}$, $\lambda_{\text{NiFe}}^{\downarrow} = 18 \text{ \AA}$, $Q_{\uparrow} = 1$, $Q_{\downarrow} = 1$, which resulted in a theoretical resistivity value of 19.8 $\mu\Omega$ cm and 8.9% of magnetoresistance amplitude, showing again, very good agreement with the experimental values. Therefore, this set of parameters is approximately equal to the one obtained for Fe 90 Å/Cu 20 Å/(NiFe 16 Å/Cu 9 Å)₂₀/NiFe 16 Å, with the exception of the $\lambda_{\text{NiFe}}^{\downarrow}$ value, which increases from 9 to 18 Å. So, the mean-free path of the majority electrons is almost the same, although there is a strong increase of transverse grain size, as mentioned above. It is also worth noting, that perfect transmission coefficients were obtained for both multilayers. In addition, the lateral size of the CCs (250 Å) for NiFe/Cu 10 Å multilayers is larger than the one obtained for a similar spin-valve sample (150 Å), as mentioned in Refs. 4 and 5. These results indicate that the change in the grain size is not a major factor in the change of the mean-free path of the majority electrons, and the scattering at the grain boundaries is not a coherent approach to explain the transport properties of various samples, and needs to be taken into account only when the mean-free path is of the order of, or larger than, the grain size. These are the reasons for the different procedures adopted in this work to fit the MR and resistivity data (a similar procedure was also used by Dieny *et al.*¹¹ in the study of NiFe/Ag multilayers), and in Refs. 4 and 5. Moreover, we are able to fit both the magnetoresistance amplitudes and resistivity values by only assuming the change of the thicknesses of the paramagnetic interfacial layers with no need to take into account any anisotropy of the mean-free path of the majority electrons.

Pettit *et al.*,²⁴ from single crystal NiFe/Cu multilayers studies, suggested that ferromagnetically coupled regions arise from pinholes in the Cu spacer layer. They argued that these coupled regions, when combined with regions of antiferromagnetic interlayer coupling and intralayer coupling, can lead to dominant biquadratic coupling. In the present work, there is no evidence of a strong biquadratic coupling as in Ref. 24, thus a predominant bilinear coupling is assumed.²⁵

E. Influence of the thickness of the Co layers at the NiFe/Cu interfaces

A series of multilayers of NiFe 54 Å/Cu 9 Å/(Co t_{Co} /NiFe 16 Å/Co t_{Co} /Cu 9 Å)₂₀/Co t_{Co} /NiFe 16 Å, with $t_{\text{Co}} = 1, 2, 3, 4, 5, 6,$ and 7 \AA , was prepared in order to study the influence of the Co thickness on the magnetic and transport properties. Parkin *et al.*⁷ have observed an enhancement of interlayer exchange coupling and a large increase of GMR by addition of thin Co interfacial layers.

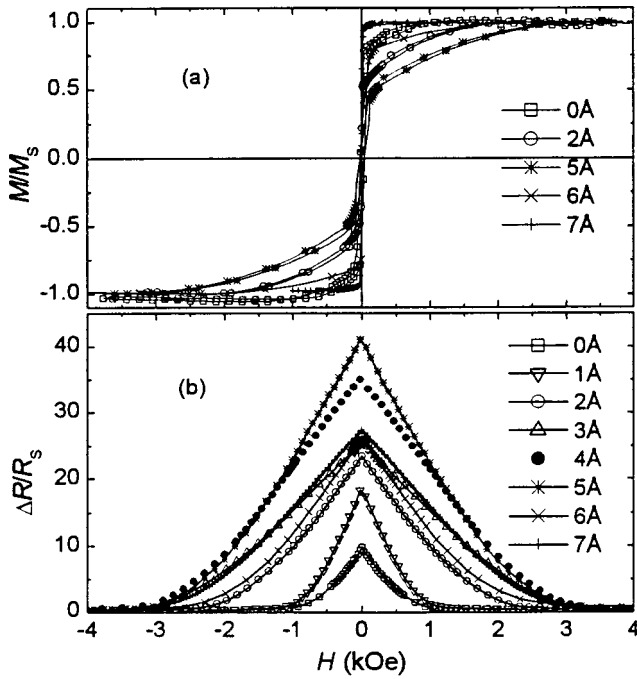


FIG. 10. (a) Magnetization curves at room temperature for a series of multilayers of composition NiFe 54 Å/Cu 9 Å/(Co t_{Co} /NiFe 16 Å/Co t_{Co} /Cu 9 Å)₂₀/Co t_{Co} /NiFe 16 Å. (b) Magnetoresistance at room temperature for the same series of multilayers.

Figure 10(a) represents hysteresis curves for some samples and Fig. 10(b) shows the magnetoresistance as a function of the applied field for all samples. One can observe a decrease of the ferromagnetic component of the magnetization curves, up to 5 Å of Co deposited at the NiFe/Cu interfaces, indicating the increase of the fraction of NiFe antiferromagnetically coupled. Above 5 Å of Co, we note an increase of the direct ferromagnetic coupling, probably caused by the presence of pinholes induced by the increase of the roughness at the interfaces, which is also responsible for the observed vanishing of MR at $t_{\text{Co}}=7$ Å (see Fig. 10).

Concerning the saturation field, one also notes an increase up to 4 Å of Co; above this thickness, the saturation field begins to decrease as a consequence of the increase of the total magnetic layer thickness [see Eq. (5)]. The existence of microscopic regions with ferromagnetic behavior can be attributed to the presence of non-negligible paramagnetic interfaces. This is produced by the small changes of the distances between the NiFe layers through the Cu layers, provoked by the intermixing between the NiFe and Cu. Since Co atoms are more immiscible in Cu than in NiFe, the role of Co deposited at the interfaces of NiFe/Cu is to avoid the intermixing between Cu and NiFe. Furthermore, it reinforces the magnetic order of the NiFe layer by substituting the nonmagnetic Cu neighbors by Co atoms.

The GMR amplitudes and resistivity were simultaneously analyzed according to the semiclassical model described in Sec. III. Rather good agreement is found between the experimental and fitting results, as shown in Fig. 11. The deduced theoretical parameters are given in Table III. Pereira *et al.*¹³ have determined the parameters for Co/Cu multilayers and we have adopted them here, even for small Co thick-

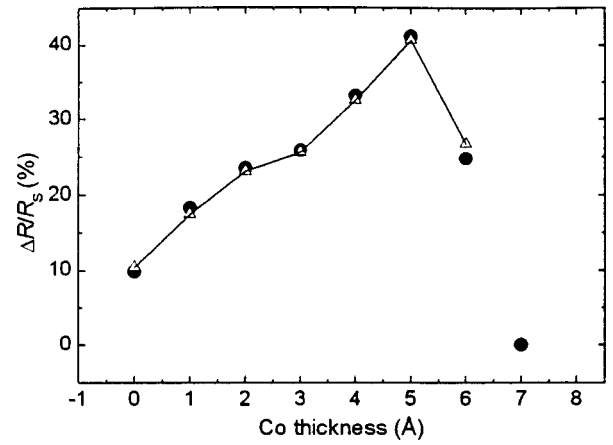


FIG. 11. GMR amplitude at room temperature dependence on Co thickness for the series of multilayers of the composition NiFe 54 Å/Cu 9 Å/(Co t_{Co} /NiFe 16 Å/Co t_{Co} /Cu 9 Å)₂₀/Co t_{Co} /NiFe 16 Å. The full circles are the experimental results and open triangles and lines are the results of the fit.

ness. The agreement between experimental and theoretical resistivity values (ferromagnetic configuration) is quite good (see Table IV). We note that Q_{\perp} decreases from 0.61 (at the NiFe/Cu interfaces) to 0.1 for $t_{\text{Co}}=1$ Å (at the Cu/Co and the NiFe/Co interfaces), indicating that the spin-dependent scattering at the interfaces begins to contribute to the GMR al-

TABLE III. Parameters deduced from the fit of both magnetoresistance and resistivity of a series of (Co t_{Co} /NiFe 16 Å/Co t_{Co} /Cu 9 Å)₂₀, where (a) represents the (Cu/Co) interfaces, (b) the (Co/NiFe) interfaces, (c) the (NiFe/Co) interfaces, and (d) the (Co/Cu) interfaces. The parameters of the temperature dependence are set as $K=1100$, $\omega=13 \times 10^{-7}$, and $\gamma=1.83$.

Co (Å)		Co <i>a</i>	NiFe <i>b</i>	Co <i>c</i>	Cu <i>d</i>
1	λ_{\uparrow} (Å)	120	95	120	180
	λ_{\downarrow} (Å)	5	5	5	180
	Q_{\uparrow}	1	0.77	0.77	1
	Q_{\downarrow}	0.1	0.1	0.1	0.1
2	λ_{\uparrow} (Å)	120	105	120	180
	λ_{\downarrow} (Å)	5	10	5	180
	Q_{\uparrow}	1	0.87	0.87	1
	Q_{\downarrow}	0.1	0.1	0.1	0.1
3	λ_{\uparrow} (Å)	120	105	120	180
	λ_{\downarrow} (Å)	5	10	5	180
	Q_{\uparrow}	1	0.91	0.91	1
	Q_{\downarrow}	0.1	0.1	0.1	0.1
4	λ_{\uparrow} (Å)	120	150	120	180
	λ_{\downarrow} (Å)	5	10	5	180
	Q_{\uparrow}	1	0.97	0.97	1
	Q_{\downarrow}	0.1	0.1	0.1	0.1
5	λ_{\uparrow} (Å)	120	220	120	180
	λ_{\downarrow} (Å)	5	1	5	180
	Q_{\uparrow}	1	1	1	1
	Q_{\downarrow}	0.1	0.1	0.1	0.1
6	λ_{\uparrow} (Å)	120	145	120	180
	λ_{\downarrow} (Å)	5	20	5	180
	Q_{\uparrow}	1	1	1	1
	Q_{\downarrow}	0.1	1	1	0.1

TABLE IV. Experimental and theoretical resistivity at saturation of a series of samples (Co t_{Co} /NiFe 16 Å/Co t_{Co} /Cu 9 Å)₂₀.

t_{Co} (Å)	1	2	3	4	5	6	7
ρ_{Exp} ($\mu\Omega$ cm)	37.3	33.7	31.0	28.6	26.2	26.6	29.5
ρ_{Fit} ($\mu\Omega$ cm)	37.3	32.8	31.6	27.7	25.5	26.8	...

ready for small Co thickness. In addition, as a result of the continuous increase of Q_{\uparrow} (at the Co/NiFe/Co interfaces) from 1 to 5 Å of Co, these interfaces present a more selective spin-dependent scattering for the electrons than the NiFe/Cu interfaces. In relation to the bulk spin-dependent scattering (in NiFe), one observes a significant increase of λ_{\uparrow} , from 70 Å (without Co) to 220 Å ($t_{\text{Co}}=5$ Å). It turns out that a fairly accurate determination of the parameters associated with the weakly scattered electrons (spin-up) can be made, while a larger uncertainty exists on the parameters associated with the strongly scattered electrons. For thickness above 5 Å of Co, λ_{\uparrow} begins to decrease, probably due to ferromagnetic coupling, which may be associated with the presence of pinholes [see Fig. 1(d) and the structural analysis shown in Sec. II]. This ferromagnetic coupling is accentuated at thicker Co thickness, resulting in a vanishing GMR amplitudes at $t_{\text{Co}}=7$ Å. It also has an influence on the resistivity values (see Table IV), with increase for Co thicknesses above 5 Å.

The maximum of MR amplitudes (41%) for Co/NiFe16 Å/Co/Cu multilayers was obtained at 5 Å of Co. This value is surprisingly high since the total magnetic layer is 26 Å thick and it shows larger MR amplitudes than the Co/Cu multilayers for similar magnetic layer thickness and number of bilayer repetitions. For instance, Kubinski and Holloway²⁶ reported a value of 12% for the amplitude of MR for (Co 30 Å/Cu 9 Å)₂₀ and Miura *et al.*²⁷ reported a value of 27% for (Co 25 Å/Cu 9 Å)₃₀. If one makes the theoretical simulation with the same parameters of Co shown in Table III, i.e., ($\lambda_{\text{Co}}^{\uparrow}=120$ Å, $\lambda_{\text{Co}}^{\downarrow}=5$ Å, $Q_{\uparrow}=1$, $Q_{\downarrow}=0.1$), 37% of MR is obtained for (Co 26 Å/Cu 9 Å)₂₀. Using the same procedure adopted by Cowache, assuming that 5 Å of Co cannot be considered thick enough to have bulk spin-dependent scattering, the theoretical simulation reproduces the experimental magnetoresistance amplitude for [(Co NiFe Co)26 Å/Cu 9 Å]₂₀, using the following parameters: ($\lambda_{\text{Co+NiFe+Co}}^{\uparrow}=165$ Å, $\lambda_{\text{Co+NiFe+Co}}^{\downarrow}=10$ Å, $Q_{\uparrow}=1$, $Q_{\downarrow}=0.1$). These results show an increase in the bulk spin-dependent scattering for the (Co NiFe Co)/Cu multilayer, larger than that in Co/Cu multilayer⁴ or in NiFe/Cu multilayer.¹⁴

Various authors studied the influence of the deposition of Co at NiFe/Cu or NiFe/Ag interfaces in sputtered spin-valve magnetoresistive structures.^{7,8,11} The increase of the MR in these structures was justified as being a result of the increase of the spin-dependent scattering occurring at the interfaces due to the increase of the magnetic ordering by the deposition of Co. In the present work, the increase of the MR amplitude is attributed to the increase of both interfacial and bulk spin-dependent scattering. We emphasize that the pair of values of the mean-free path (220 and 1 Å) in NiFe results in a more selective spin-dependent scattering in the bulk,

when compared to other values reported in the literature.^{3,11,14,22,28}

V. CONCLUSIONS

We have shown that the presence of an interfacial paramagnetic layer at the NiFe/Cu interfaces masks the estimated mean-free path of both types of electrons because their effective values are reduced mainly for small NiFe thickness. The influence of the buffer layer (Fe or NiFe) on the magnetoresistive properties for NiFe/Cu multilayers has been investigated. The transmission coefficients, deduced from the calculation, decrease when the Fe buffer layer is replaced by a NiFe one. This result is interpreted in terms of the variations of the interfacial intermixing and roughness at the interfaces, leading to an increase of the paramagnetic interfacial layer thickness. The scattering within these layers is not spin dependent and reduces the MR amplitude. Concerning the field sensitivity of NiFe/Cu multilayers, it increases continuously from 11 to 85 Å of NiFe, although the largest amplitude of MR is obtained for small NiFe thickness (21 Å). The effect of the Co deposition at the NiFe/Cu interfaces has also been investigated. The maximum MR amplitudes (41%) for Co/NiFe16 Å/Co/Cu multilayers is obtained at 5 Å of Co. The increase of the MR amplitude is partially attributed to the increase of the interfacial spin-dependent scattering. This is due to a more selective transmission of the electrons through the interfaces associated with the increase of the magnetic order at the NiFe/Co and Co/Cu interfaces. We showed that an increase of the bulk NiFe spin-dependent scattering must be considered as well. This effect is attributed to the reduction of the paramagnetic interfacial layer thickness, and as a consequence, a larger effective NiFe thickness can contribute to the bulk spin-dependent scattering.

ACKNOWLEDGMENTS

The authors wish to thank A. Morrone for the technical support during the experiments; Dr. J. Geshev for critical reading of the manuscript; and CNPq, FAPERJ, and FAPERGS for partial support of this work. One of the authors (L.C.C.M.N.) thanks PCI/MCT, which supported his one month stay at CBPF for the preparation of the samples.

¹T. Lucinski *et al.*, J. Magn. Magn. Mater. **174**, 192 (1997).

²J. Dubowik, F. Stobiecki, and T. Lucinski, Phys. Rev. B **57**, 5955 (1998).

³V. S. Speriosu *et al.*, Phys. Rev. B **47**, 11579 (1993).

⁴B. Dieny, Europhys. Lett. **17**, 261 (1992).

⁵B. Dieny *et al.*, in *Magnetism and Systems of Reduced Dimensions*, edited by Farrow *et al.* (Plenum, New York, 1993).

⁶Z. T. Diao, S. Goto, K. Meguro, and S. Tsunashima, J. Appl. Phys. **81**, 2327 (1997).

⁷S. S. P. Parkin, Appl. Phys. Lett. **61**, 1358 (1992).

⁸S. S. P. Parkin, Phys. Rev. Lett. **71**, 1641 (1993).

⁹Th. G. S. M. Rijks *et al.*, IEEE Trans. Magn. **31**, 3865 (1995).

¹⁰A. R. Modak, D. J. Smith, and S. S. P. Parkin, Phys. Rev. B **50**, 4232 (1994).

¹¹C. Cowache *et al.*, Phys. Rev. B **53**, 15027 (1996).

¹²R. E. Camley and J. Barnas, Phys. Rev. Lett. **63**, 664 (1989).

¹³L. G. Pereira, J. L. Duvail, and D. K. Lottis, J. Appl. Phys. **88**, 4772 (2000).

¹⁴B. Dieny *et al.*, J. Magn. Magn. Mater. **151**, 378 (1995).

- ¹⁵E. E. Fullerton *et al.*, Phys. Rev. Lett. **68**, 859 (1992).
- ¹⁶S. S. P. Parkin *et al.*, Phys. Rev. Lett. **72**, 3718 (1994).
- ¹⁷B. Rodmacq, K. Dumesnil, P. Mangin, and M. Hennion, Phys. Rev. B **48**, 3356 (1993).
- ¹⁸A. Barthelmy *et al.*, J. Appl. Phys. **67**, 5908 (1990).
- ¹⁹R. M. Bozorth, *Ferromagnetism* (Van Nostrand, New York, 1956).
- ²⁰L. C. C. M. Nagamine *et al.*, J. Magn. Magn. Mater. **195**, 437 (1999).
- ²¹C. Wivel and S. Morup, J. Phys. E **14**, 605 (1981).
- ²²L. C. C. M. Nagamine *et al.*, J. Magn. Magn. Mater. **242**, 541 (2002).
- ²³H. P. Sun *et al.*, J. Appl. Phys. **87**, 2835 (2000).
- ²⁴K. Petit, S. Gider, S. S. P. Parkin, and M. B. Salomon, Phys. Rev. B **56**, 7819 (1997).
- ²⁵The presence of the pinholes is not very likely to occur for the Cu thickness corresponding to the second peak of the antiferromagnetic coupling. However, in our studies on NiFe/Cu and Co/NiFe/Co/Cu multilayers, with $t_{\text{Cu}}=20 \text{ \AA}$ (not published), we have obtained a similar influence of the paramagnetic interfacial layers on the magnetic and magnetoresistive properties as these presented here. Therefore, these additional results are in tune with our interpretation of the experimental data, showing a strong influence of the paramagnetic interfacial layers.
- ²⁶D. J. Kubinski and H. Holloway, J. Appl. Phys. **79**, 7395 (1996).
- ²⁷S. Miura *et al.*, J. Appl. Phys. **85**, 4463 (1999).
- ²⁸B. A. Gurney *et al.*, Phys. Rev. Lett. **71**, 4023 (1993).